

Realization of Bose-Einstein condensates in lower dimensions

A. Görlitz, J. M. Vogels, A. E. Leanhardt, C. Raman, T. L. Gustavson, J. R. Abo-Shaeer, A. P. Chikkatur, S. Gupta, S. Inouye, T. P. Rosenband, D. E. Pritchard, W. Ketterle
*Department of Physics and Research Laboratory of Electronics,
 Massachusetts Institute of Technology, Cambridge, MA 02139*

(November 26, 2024)

Bose-Einstein condensates of sodium atoms have been prepared in optical and magnetic traps in which the energy-level spacing in one or two dimensions exceeds the interaction energy between atoms, realizing condensates of lower dimensionality. The cross-over into two-dimensional and one-dimensional condensates was observed by a change in aspect ratio and saturation of the release energy when the number of trapped atoms was reduced.

New physics can be explored when the hierarchy of physical parameters changes. This is evident in dilute gases, where the onset of Bose-Einstein condensation occurs when the thermal deBroglie wavelength becomes longer than the average distance between atoms. Dilute-gas condensates of density n in axially-symmetric traps are characterized by four length scales: Their radius R_{\perp} , their axial half-length R_z , the scattering length a which parameterizes the strength of the two-body interaction, and the healing length $\xi = (4\pi na)^{-1/2}$. In almost all experiments on Bose-Einstein condensates, both the radius and length are determined by the interaction between the atoms and thus, $R_{\perp}, R_z \gg \xi \gg a$. In this regime, a BEC is three-dimensional and is well-described by the so-called Thomas-Fermi approximation [1]. A qualitatively different behavior of a BEC is expected when the healing length is larger than either R_{\perp} or R_z since then the condensate becomes restricted to one or two dimensions, respectively. New phenomena that may be observed in this regime are for example quasi-condensates [2–4] and a Tonk’s gas of impenetrable bosons [4–6].

In this Letter, we report the experimental realization of cigar-shaped one-dimensional condensates with $R_z > \xi > R_{\perp}$ and disk-shaped two-dimensional condensates with $R_{\perp} > \xi > R_z$. The cross-over from 3D to 1D or 2D was explored by reducing the number of atoms in condensates which were trapped in highly elongated magnetic traps (1D) and disk-shaped optical traps (2D) and measuring the release energy. In harmonic traps, lower dimensionality is reached when $\mu_{3D} = 4\pi\hbar^2 a n/m < \hbar\omega_t$. Here, ω_t is the trapping frequency in the tightly confining dimension(s) and μ_{3D} is the interaction energy of a weakly interacting BEC, which in 3D corresponds to the chemical potential. Other experiments in which the interaction energy was comparable to the level spacing of the confining potential include condensates in one-dimensional optical lattices [8] and the cross-over to an ideal-gas (zero-D) condensate [7], both at relatively low numbers of condensate atoms.

Naturally, the number of interacting atoms in a lower-

dimensional condensate is limited. The peak interaction energy of a 3D condensate of N atoms with mass m is given by $\mu_{3D} = \hbar^2/2m (15Na/l_z^2 l_{\perp}^4)^{2/5}$, where $l_{\perp, z} = (\hbar/m\omega_{\perp, z})^{1/2}$ are the oscillator lengths of the harmonic potential. The cross-over to 1D and 2D, defined by $\mu_{3D} = \hbar\omega_t$ or equivalently $\xi = l_t$ occurs if the number of condensate atoms becomes

$$N_{1D} = \sqrt{\frac{32\hbar}{225ma^2}} \sqrt{\frac{\omega_{\perp}}{\omega_z^2}} = \sqrt{\frac{\omega_{\perp}}{\omega_z^2}} \times 7200 \sqrt{\frac{\text{rad}}{\text{s}}} \quad (1)$$

$$N_{2D} = \sqrt{\frac{32\hbar}{225ma^2}} \sqrt{\frac{\omega_z^3}{\omega_{\perp}^4}} = \sqrt{\frac{\omega_z^3}{\omega_{\perp}^4}} \times 7200 \sqrt{\frac{\text{rad}}{\text{s}}}, \quad (2)$$

where we have used the scattering length ($a = 2.75$ nm) and mass of ^{23}Na atoms to derive the numerical factor. Our traps feature extreme aspect ratios resulting in $N_{1D} > 10^4$ and $N_{2D} > 10^5$ while for most standard BEC traps the numbers are significantly smaller.

For a 1D condensate the condition $\xi = l_t$ yields a linear density $\tilde{n}_{1D} \approx 1/4a$, implying that the linear density of a 1D condensate is limited to less than one atom per scattering length independent of the radial confinement. Therefore, tight transverse confinement, as may be achievable in small magnetic waveguides [9] or hollow laser beam guides [10], is by itself not helpful to increase the number of atoms in a 1D condensate. Large 1D numbers may only be achieved at the expense of longer condensates or if the scattering length is smaller.

In anisotropic traps, a primary indicator of crossing the transition temperature for Bose-Einstein condensation is a sudden change of the aspect ratio of the ballistically expanding cloud, and an abrupt change in its energy. The transition to lower dimensions is a smooth cross-over, but has similar indicators. In the 3D Thomas-Fermi limit the degree of anisotropy of a BEC is independent of the number N of atoms, whereas in 1D and 2D, the aspect ratio depends on N . Similarly, the release energy in 3D depends on N [1] while in lower dimensions, it saturates at the zero-point energy of the tightly confining dimension(s), when N becomes smaller.

A trapped 3D condensate has a parabolic shape and its radius and half-length are given by $R_{\perp} = l_{\perp}(15Nal_{\perp}/l_z^2)^{1/5}$ and $R_z = l_z(15Nal_z^3/l_{\perp}^4)^{1/5}$ [1], resulting in an aspect ratio of $R_{\perp}/R_z = l_{\perp}^2/l_z^2 = \omega_z/\omega_{\perp}$. When the 2D regime is reached by reducing the atom number, the condensate assumes a Gaussian shape with an rms width $\approx l_z$ along the axial direction, but retains the parabolic shape radially. The radius of a trapped 2D condensate decreases with N as $R_{\perp} = (128/\pi)^{1/8}(Nal_{\perp}^4/l_z)^{1/4}$ [3]. Similarly, the half-length of trapped 1D condensates is $R_z = (3Nal_z^4/l_{\perp}^2)^{1/3}$ [4].

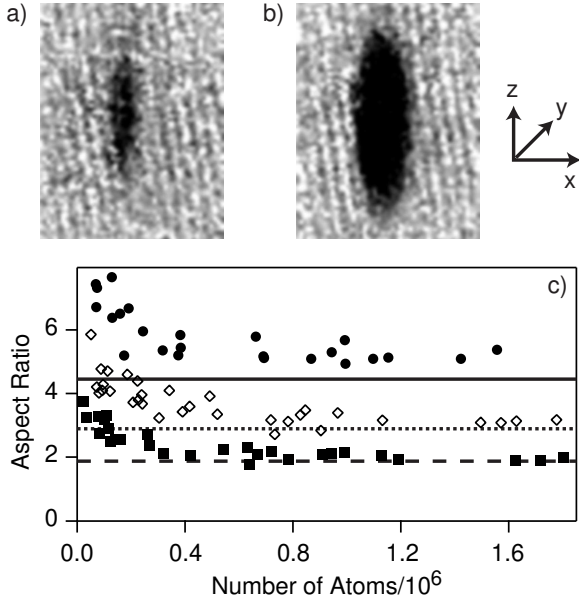


FIG. 1. Cross-over from 3D to 2D condensates observed in the change of the aspect ratio. Condensates were released from a disk-shaped optical trap and observed after 15 ms time-of-flight. a) (2D) condensate with 9×10^4 atoms b) (3D) condensate with 8×10^5 atoms in a trap with vertical trap frequency of $\omega_z/2\pi \approx 790$ Hz. c) Aspect ratio as a function of atom number for optical traps with vertical trap frequencies of 1620 Hz (filled circles), 790 Hz (open diamonds) and 450 Hz (filled squares). The lines indicate the aspect ratios as expected for condensates in the 3D (Thomas-Fermi) regime. We attribute discrepancies between expected and measured aspect ratio for large numbers to the influence of anharmonicities on the measurement of the trap frequencies.

Our experiments in which one- and two-dimensional Bose-Einstein condensates were realized were carried out in two different experimental setups. For the study of condensates in a 2D geometry, condensates of $\approx 10^7$ atoms were generated as described in Refs. [11,12] and transferred into an optical trap [13]. The optical trapping potential was generated by focusing a 1064 nm laser into a light sheet using cylindrical lenses, with the tight focus in the vertical dimension to provide optimum support against gravity. This resulted in typical trap frequencies of $\omega_z/2\pi = 790$ Hz, $\omega_{\perp x}/2\pi = 30$ Hz and $\omega_{\perp y}/2\pi = 10$ Hz

for a laser power of ≈ 600 mW. The transfer from the magnetic trap into the optical trap was accomplished by turning on the trapping light field and turning down the magnetic trapping potential resulting in a transfer efficiency of more than 50%. The depth of the optical potential and the trap frequencies could be easily varied by changing the power of the trapping beam.

To observe the transition from the 3D Thomas-Fermi regime into a 2D situation, we have adjusted the number of condensate atoms between 2×10^6 and 3×10^4 by exposing the optically trapped BEC to a thermal sodium atomic beam. Condensates were detected by suddenly releasing the atoms from the trap and taking absorption images after 15 ms free expansion. The condensates dropped by $15 \mu\text{m}$ during the $100 \mu\text{s}$ imaging time, which is less than 10% of the measured length of our shortest condensates. During expansion, the interaction energy is converted almost exclusively into kinetic energy in the tightly confining vertical direction. Thus, the vertical length of the condensate expands quickly while the horizontal dimensions almost retain their size in the trap. The aspect ratio changes dramatically, and for the chosen time-of-flight the axial dimension is even larger than the radial one. The aspect ratio was determined by fitting the condensate with a parabolic Thomas-Fermi distribution which is exact in the large-number limit. For small numbers the vertical condensate shape approaches a Gaussian, but we also used the parabolic fitting function to avoid any bias. A parabolic fitting function may underestimate the rms width of a Gaussian by at most 20%.

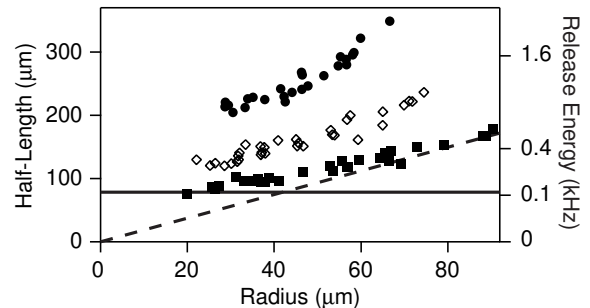


FIG. 2. Saturation of the half-length and correspondingly the release energy at the cross-over from 3D to 2D for the same optical traps as in Fig.1. The dashed line represents the expected behavior of a purely 3D condensate and the solid line the expected saturation level of the release energy for the weakest trap (filled squares).

Figures 1a,b show how the expanded condensate became more elongated for small atom numbers, clear evidence for reaching 2D. In Fig. 1c the aspect ratio of condensates in three different optical traps is shown. For all our trap parameters, the aspect ratio approaches a constant value for large atom numbers, which can be calculated using the results of [14] for the Thomas-Fermi

limit. The increase of the aspect ratio for small atom numbers is due to clamping of the vertical length of the condensate because of saturation of the release energy while the width shrinks further. For the weakest trap, using Eq. 2, $N_{2D} = 2.9 \times 10^5$, while we could observe condensates with as low as $N_{2D}/10$.

The saturation of the mean release energy per particle at the kinetic part of the zero-point energy of the trap becomes obvious if the half-length of the expanded condensates is plotted versus the radius (see Fig. 2). For a long enough time-of-flight, the mean release energy is simply proportional to the square of the measured half-length and is given by $E_{rel} = mR_z(t)^2/14t^2$. In all our traps the half-length appears to saturate at a value which corresponds to a release energy close to $\hbar\omega_z/4$ which is the vertical kinetic zero-point energy.

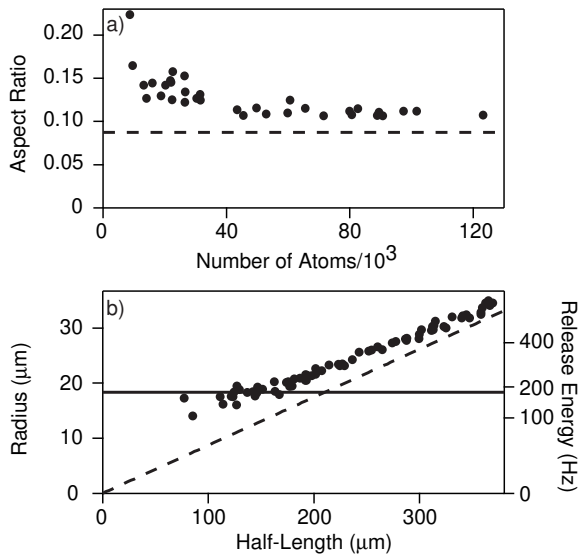


FIG. 3. Crossover from 3D to 1D condensates. a) Aspect ratio in time-of-flight images versus the number of atoms. b) Radial versus axial size for the same time-of-flight data, showing saturation of the release energy at close to the expected value (solid line). The dashed line represents the behavior of a 3D condensate. Note, that the use of a parabolic fitting function slightly underestimates the release energy in the 1D regime.

The 1D experiments were carried out in a Ioffe-Pritchard type magnetic trap with radial and axial trapping frequencies of $\omega_{\perp}/2\pi = 360$ Hz and $\omega_z/2\pi = 3.5$ Hz [15]. We obtained an extreme aspect ratio of ~ 100 by reducing the axial confinement during the final evaporation stage. As in the 2D case, the number of atoms in the condensate was lowered by exposing the gas to a thermal sodium beam, followed by a reequilibration time of 15 s. A radio-frequency shield [12] limited the trap depth to 20 – 40 kHz (1 – 2 μ K). We analyzed the cloud using absorption imaging along one of the radial directions after a ballistic expansion of $t = 4$ ms. In con-

trast to the 2D experiments, the aspect ratio of the cloud was not yet inverted after this short time-of-flight. The measured condensate sizes were corrected for the finite imaging resolution of $5\mu\text{m}$, a correction of less than 10%.

Similar to the 2D experiment, the cross-over to the 1D regime was observed by a change of the aspect ratio when the number of atoms was reduced (Fig. 3). In the 3D limit, neglecting the initial radial size and the axial expansion (both $< 1\%$ corrections) the aspect ratio equals $\omega_z t$ independent of N . The deviation from this behavior below $\approx 5 \times 10^4$ atoms demonstrates the cross-over to 1D behavior. At the same time, the release energy saturated at $\hbar\omega_{\perp}/2$, the zero-point kinetic energy of the trapping potential (Fig. 3b). For this trap, Eq. 1 yields $N_{1D} = 1.6 \times 10^4$, while we could observe condensates with as low as $N_{1D}/2$. In the 1D geometry, the aspect ratio deviates from the 3D limit for larger ratios of N/N_{1D} than in the 2D case, since the interaction energy per particle at the cross-over to 1D is only approximately half the kinetic zero-point energy while at the cross-over to 2D, it is roughly equal to the kinetic zero-point energy.

So far, we have discussed only the condensate and its cross-over from the Thomas-Fermi regime into a lower-dimensional situation. Here, we will briefly address the thermal component and finite temperature effects. The finite trap depth U_{trap} provides constant evaporative cooling which counteracts any residual heating and stabilizes the temperature. The equilibrium temperature in both the 1D and 2D experiment can be estimated to be a constant fraction $1/\eta$ of the trap depth U_{trap} . For a quantum saturated thermal cloud ($T < T_c$), the number of thermal atoms N_{th} can be approximated by simply counting the number of states with an energy below $k_B T$, which results in $N_{\text{th}} \approx (U_{\text{trap}}/\eta\hbar)^3/\omega_{\perp}^2\omega_z$. This estimate assumes that the thermal cloud is still three-dimensional ($k_B T > \hbar\omega_{\perp,z}$), in agreement with the situation in the experiment. To be able to discern the condensate from the thermal cloud, N_{th} should not be much larger than N_{1D} (N_{2D}). This simple argument implies that for our 1D trap where $N_{1D} \approx 1.6 \times 10^4$, the maximum allowed trap depth would be 60 kHz assuming a typical $\eta = 10$ and a minimum condensate fraction of 10%. This is in fair agreement with our experimental observations.

In a magnetic trap, the trap depth can be adjusted independently of the trap frequencies using an rf shield. In an optical trap created using a single Gaussian focus, the trap frequencies are proportional to the square root of the trap depth. Thus, tighter optical traps can store more thermal atoms, yet Eq. 2 implies that N_{2D} is lower for tighter traps. Therefore, tight single-focus optical traps are less suitable for the observation of lower-dimensional condensates. Experimentally, we have observed that for weaker traps we could penetrate further into the 2D regime (see Fig. 1c) than for tighter ones, which is consistent with the considerations above.

In our experiments, the thermal cloud is always three-

dimensional, which necessarily requires that the critical temperature T_c for Bose condensation is also larger than the energy level spacing of the trap, i.e. $k_B T_c > k_B T > \hbar\omega_t$. A new physical regime in which the condensation process could be studied in lower dimensions would be reached if thermal excitations freeze out before a BEC forms. This requires that the total number of atoms N be smaller than the number of states with an energy smaller than $\hbar\omega_t$. Thus, in 1D, the number of atoms may not exceed the aspect ratio of the trap, i.e. $N < A = \omega_t/\omega_w$, where ω_w is the trapping frequency in the weakly confining direction, while in 2D the relevant criterion is $N < A^2$. For the traps used in our experiments, this implies $N < 100$ (1D) or $N < 2500$ (2D), which, at least for 2D, seems to be within experimental reach. The physics of Bose-condensation in 2D has been discussed in several publications. It is not yet clear under what circumstances one will observe quasi-condensates [2,3] or the Kosterlitz-Thouless transition [16]. A full understanding of the observation of 2D quantum degeneracy of spin-polarized hydrogen [17] is still lacking, and controlled experiments with dilute gases could give useful insights. In a 1D geometry a related effect that could be observed is a two-step condensation as discussed in [20].

Lower-dimensional condensates, as prepared in our experiments, offer many opportunities for further scientific studies. Topological excitations such as solitons (in 1D) and vortices (in 2D) should be much more stable than in 3D, where solitons suffer from kink instabilities and vortices can bend. The character and spectrum of the collective excitations is expected to exhibit a qualitative change in lower dimensions [18].

Another area of significant theoretical interest is the study of phase fluctuations [2–4] and its relation to the formation of quasi-condensates, which locally behave like ordinary condensates but do not have a globally uniform phase. In 3D, the energy associated with such phase fluctuations is usually higher than $k_B T_c$ (except for very extreme aspect ratios), whereas in 1D and 2D it can be lower. It might be possible to observe the phase fluctuations by observing a broadening of the Doppler spectrum of the condensate [19].

An even more ambitious goal is the observation of a Tonks gas in a one-dimensional geometry [5,4,6]. At zero temperature, such a gas of “impenetrable bosons” is realized when the axial distance $1/\tilde{n}$ between atoms exceeds the 1D healing length, $\xi = l_\perp/(2\tilde{n}a)^{1/2}$ [4], resulting in $\tilde{n}_{\text{Tonks}} = 2a/l_\perp^2$ as a condition for the linear density. Thus, \tilde{n}_{Tonks} is $8a^2/l_\perp^2$ times smaller than \tilde{n}_{1D} . In 2D, the collision physics is severely altered only for $a/R_z > 1$ [3]. Such regimes require much tighter confinement than in our experiment and may be realized using optical lattices or magnetic microtraps, or alternatively a larger scattering length, for example near a Feshbach resonance.

In conclusion, we have prepared lower-dimensional

condensates in optical and magnetic traps. The cross-over into lower-dimensional behavior was indicated by a change in the aspect ratio of the cloud and a saturation of the release energy as the condensate number was lowered. Due to the extreme geometries of our traps the number of atoms at the cross-over to lower-dimensionality is rather large ($> 10^5$ in the 2D case) which provides a good starting point for the exploration of phenomena which only occur in one or two dimensions.

This research is supported by NSF, ONR, ARO, NASA, and the David and Lucile Packard Foundation. A. E. L. and A. P. C. acknowledge additional support by a fellowship from NSF and JSEP, respectively.

-
- [1] F. Dalfovo, S. Giorgini, L. P. Pitaevskii, and S. Stringari, *Rev. Mod. Phys.* **71**, 463 (1999).
 - [2] Y. Kagan, B. V. Svistunov, and G. V. Shlyapnikov, *Sov. Phys. JETP* **66**, 314 (1987).
 - [3] D. S. Petrov, M. Holzmann, and G. V. Shlyapnikov, *Phys. Rev. Lett.* **84**, 2551 (2000).
 - [4] D. S. Petrov, G. V. Shlyapnikov, and J. T. M. Walraven, *Phys. Rev. Lett.* **85**, 3745 (2000).
 - [5] L. Tonks, *Phys. Rev.* **50**, 955 (1936).
 - [6] M. Olshanii, *Phys. Rev. Lett.* **81**, 938 (1998).
 - [7] M. Holland, D. S. Jin, M. L. Chiofalo, and J. Cooper, *Phys. Rev. Lett.* **78**, 3801 (1997).
 - [8] C. Orzel *et al.* *Science* **291**, 2386 (2001).
 - [9] J. Fortagh, A. Grossmann, C. Zimmermann, and T. W. Hänsch, *Phys. Rev. Lett.* **81**, 5310 (1998); J. Reichel, W. Hänsel, and T. W. Hänsch, *ibid.* **83**, 3398 (1999); D. Müller *et al.*, *ibid.* **83**, 5194 (1999); N. H. Dekker *et al.*, *ibid.* **84**, 1124 (2000); M. Key *et al.*, *ibid.* **84**, 1371 (2000) R. Folman *et al.*, *ibid.* **84**, 4749 (2000).
 - [10] T. Kuga *et al.*, *Phys. Rev. Lett.* **78**, 4713 (1997); K. Bongs *et al.*, *Phys. Rev. A* **63**, 031602(R) (2001).
 - [11] M. O. Mewes *et al.*, *Phys. Rev. Lett.* **77**, 416 (1996).
 - [12] W. Ketterle, D. S. Durfee, and D. M. Stamper-Kurn, in *Bose-Einstein condensation in atomic gases, Proceedings of the International School of Physics Enrico Fermi, Course CXL*, edited by M. Inguscio, S. Stringari, and C. Wieman (IOS Press, Amsterdam, 1999), pp. 67–176.
 - [13] D. M. Stamper-Kurn *et al.*, *Phys. Rev. Lett.* **80**, 2027 (1998).
 - [14] Y. Castin and R. Dum, *Phys. Rev. Lett.* **77**, 5315 (1996).
 - [15] R. Onofrio *et al.*, *Phys. Rev. Lett.* **84**, 810 (2000).
 - [16] W. J. Mullin, M. Holzmann, and F. Laloe, *J. Low Temp. Phys.* **121**, 263 (2000).
 - [17] A. I. Safonov *et al.*, *Phys. Rev. Lett.* **81**, 4545 (1998).
 - [18] T. L. Ho and M. Ma, *JLTP* **115**, 61 (1999).
 - [19] J. Stenger *et al.*, *Phys. Rev. Lett.* **82**, 4569 (1999); E. W. Hagley *et al.*, *ibid.* **83**, 3112 (1999).
 - [20] W. Ketterle and N. J. van Druten, *Phys. Rev. A* **54**, 656 (1996).